MAGNON DRAG EFFECT ON RESISTIVITY AND THERMOELECTRIC POWER OF SEMIMETALLIC ANTIFERROMAGNET USb

Z. HENKIE AND P. WIŚNIEWSKI

W. Trzebiatowski Institute of Low Temperature and Structure Research
Polish Academy of Sciences
P.O. Box 937, 50-950 Wrocław 2, Poland

(Received August 23, 1994; revised version June 19, 1995)

Resistivity $\rho(T)$ and absolute thermoelectric power $S(T)$ have been measured for USb single crystals characterized by different residual resistivity ratios, $RRR = \rho(300\ \mathrm{K})/\rho(4.2\ \mathrm{K})$. A 50 μV/K peak of $S(T)$ observed at 40 K for high RRR crystal vanishes for low RRR one. The $\rho \propto T^4$ dependence observed below 40 K changes to the $\rho \propto T^{5/2}$ one. These variations are ascribed to reduction of the magnon drag effect by an increased incoherent magnetic scattering of carriers, possibly induced by a small change of composition. Resistivity anomaly is analysed above the antiferromagnetic transition temperature T_N. We have found that resistivity decreases as $t \ln t$ in the range $0.02 \leq t \leq 0.35$, where $t = (T - T_N)/T_N$. It is ascribed to a semimetallic character of this compound.

PACS numbers: 72.20.Pa, 72.15.Jf, 72.15.Eb, 75.50.Ee

1. Introduction

Though USb is one of the best examined uranium compounds [1, 2], it still draws a continuous interest. Cooper et al. [3] showed that hybridization of U–5f electrons to conduction band electrons leads to a diminution of the ordered magnetic moment and a fluctuating 5f spectral admixture into the conduction bands. It also makes the magnetic properties of uranium ions sensitive to a change of their chemical environment. The aim of this work is to examine the sample dependence of the temperature dependent resistivity and thermoelectric power.

USb has an fcc (NaCl type) crystal structure and shows triple-$\boldsymbol{k}$ antiferromagnetic ordering below $T_N = 213$ K [4]. On the basis of previous resistivity, Hall effect [5, 6] and magnetooptical studies [7] the USb was characterized as a semimetallic Kondo lattice system with the f–d electrons interaction integral $J_{df} = -0.18$ eV and the conduction electrons concentration below 0.1 e/f.u. (formula unit). Its thermoelectric power, equal to 41 μV/K [8] at ambient temperature, becomes negative below 150 K and shows a peak of about 5 μV/K at *ca.* 40 K. An

interest in transport properties of USb has been renewed recently in consequence of quality improvement of USb crystals prepared for de Haas–van Alphen effect examination [9, 10].

2. Sample preparation and characterization

USb single crystals, grown in two experiments by the chemical vapour transport method [11], were used to prepare samples of dimensions of about $0.5 \times 0.5 \times 3$ mm^3, with the length going along *ca.* [100] crystal axis for samples A and B, and along [110] for sample C.

The samples A and B were examined by scanning electron microscope with an energy dispersive X-ray microanalysis. Their lattice parameters were determined by the standard X-ray powder diffraction. The ratio of uranium content in sample A, (U_A), to that in sample B, (U_B), is equal to $U_A/U_B = 0.985 \pm 0.011$. The lattice constant a is equal to 6.198 ± 0.002 Å and 6.205 ± 0.002 Å, while the Néel temperature is equal to 211.2 K and 218.7 K for samples A and B, respectively. The values of the lattice constant can be compared to $a = 6.210$ Å reported for high quality USb crystals in Refs. [9, 10]. In the latter case the authors have noticed that annealing accompanied with evaporation of the Sb excess increases *RRR* from 18 to 38 [10]. The powder X-ray diagrams are of the same quality for both crystals though the macrostructure of crystal A is clearly better as judged from the better form of natural crystal faces and edges as well as from a better quality of the Laue picture. *RRR* for crystal A (equal to 1.6) is unexpectedly lower than that for crystal B (equal to 13). However we conclude from our data and from observation of Hotta et al. [10] that the increase in both *RRR* and the lattice constant, in the *RRR* range from 1.6 to 38, is at least partially due to a decrease in Sb excess.

The resistivity has been measured by the conventional four-point dc method. The method for thermoelectric power measurements is given in Ref. [12]. Critical behaviour of the resistivity has been examined on sample C characterized by $T_N = 210.3$ K.

3. Results

The resistivity data are plotted versus T/T_N in Fig. 1. The earlier data of Schoenes et al. [5] are shown by the broken line. Our $\rho(T)$ data were multiplied by constant factors in order to meet the data of Schoenes et al. [5] at $T/T_N = 1$. The mean value of the room temperature resistivities for samples A and B equals 580 $\mu\Omega$ cm. The individual values differ from each other by *ca.* 10%, i.e. less than geometrical factor inaccuracy (*ca.* 15%). For all the samples the dependence ρ versus T/T_N is nearly identical above $T_{max}/T_N = 0.63$ (maximum of $\rho(T)$) and different at lower temperatures. On the other hand the recent resistivity data showed a decrease in $\rho(T_{max})$ by nearly 10%, when $RRR \sim 15$ of the as-grown crystal was about twice increased due to annealing [9, 10].

Figure 2 shows the $S(T)$ data. $S(300\text{ K})$ is equal to 38.8 μV/K and 42.1 μV/K for samples A and B, respectively. An abrupt change of the $S(T)$ slope determines T_N. The thermoelectric power sign change is observed at $T_S \approx T_{max}$. T_S equals 131 K and 149 K for samples A and B, respectively. The sign change of the Hall coefficient was observed by Schoenes et al. [5] at about 110 K.

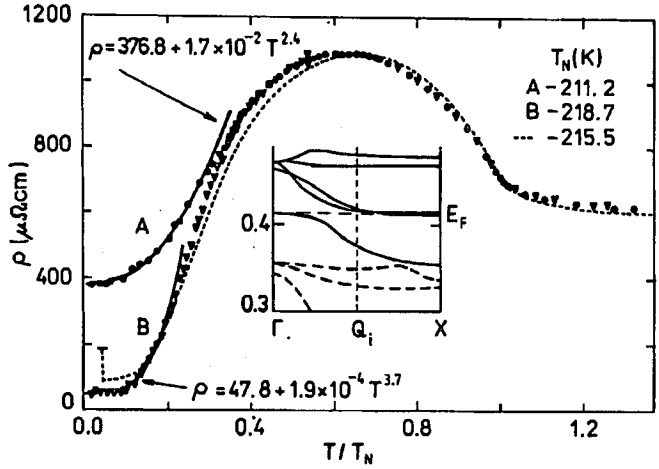

Fig. 1. Temperature dependence of resistivity for two crystals of USb (this work) — full circles and triangles, compared to that of Ref. [5] — broken line. The vertical broken bar gives a range of residual resistivity observed in Ref. [5]. The inset shows a fragment of the band structure from Ref. [13]. Copyright by Elsevier Science Publishers (reproduced with permission).

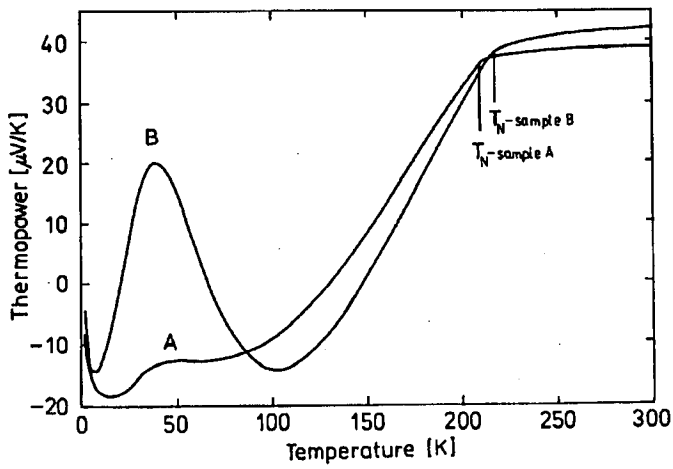

Fig. 2. Thermoelectric power for USb crystals: A and B.

A huge peak of the thermoelectric power at about 40 K is observed for sample B. A slight reminiscence of this peak is observed for sample A. Another feature that should be stressed is the strong $S(T)$ dependence below 3.5 K ($\mathrm{d}S/\mathrm{d}T \approx 5\ \mu\mathrm{V/K^2}$).

4. Discussion

4.1. Effect of antiferromagnetic ordering

The resistivity behaviour for USb is qualitatively consistent with that predicted for antiferromagnetic metals; the resistivity decreases when T increases through T_N [14]. The anomaly for USb, however, is highly enhanced. Schoenes et al. [5] suggested that the enhancement is due to the semimetallic character of USb. That suggestion is consistent with the similar type resistivity behaviour found for NpAs, which has the same magnetic and crystal structure but the carrier concentration by over one order lower [15].

On the other hand a qualitatively similar and also strongly enhanced anomaly of $\rho(T)$ was observed for UP_2 and USb_2 [16] along the easy magnetic direction. These two uniaxial antiferromagnets show metal-like carrier concentrations equal to 1.2 and 0.53 e/f.u. [17], respectively. They do not show, however, the change of thermoelectric power sign below T_N, which was observed for USb [8]. Therefore, we have quantitatively examined $\rho(T)$ above T_N.

We follow in our analysis the notation used in Ref. [18] and describe resistivity in terms of the following equation

$$R = \frac{T_N}{\rho_\infty}\rho(T) = At^{1-\alpha} + Bt + C, \qquad t = (T - T_N)/T_N \tag{1}$$

in the $210.5 < T < 214.8$ K range (Fig. 3). The resistivity at ambient temperature was taken as a high temperature limit of the spin disorder resistivity ρ_∞.

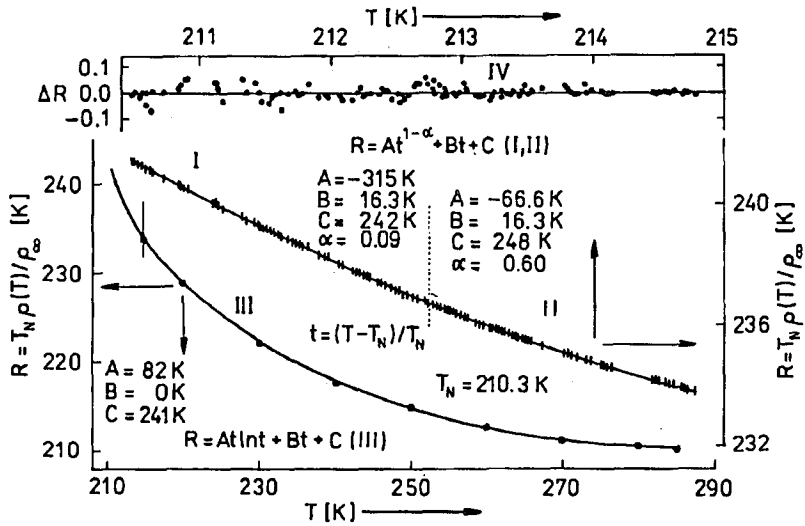

Fig. 3. Temperature dependence of resistivity along ⟨110⟩ crystal axis of USb having $T_N = 210.3$ K. The solid curves present our best fit of Eq. (I,II) to the data in the ranges I and II; Eq. (III) - in the range III. Corresponding parameters are given in a rounded up form. Points IV give a deviation of the data from the function (I, II).

The data were analysed using a nonlinear least squares method to fit the experimental data to Eq. (1). The effect of the temperature range of the fit on the value of the fitted parameters has been examined. At some temperatures the rapid change of fitted parameters is observed. There are three ranges in the temperature interval between 210.5 K and the room temperature. The best fit of Eq. (1) to the experimental data in the lowest temperature range, $1 \times 10^{-3} < t < 1.15 \times 10^{-2}$, is obtained for $T_N = 210.3$ K, chosen so as α and T_N have the same value below and above this T_N. This value of T_N has also been used for two other ranges.

In two first ranges the confidence to the fitted parameters was poor when all of them were left free. It was because of the weak sensitivity of the fit on the value of B. Therefore, this parameter has been fixed when the others were left free during fitting. We have inspected the value of B from 16.33 K to 3.27 K. They were estimated by assuming that at the temperature of 1000 K the USb resistivity [6] is either dominated by phonon resistivity or that the phonon contribution amounts merely 20% of total resistivity (that is the common case for uranium compounds — see for instance UN) [19].

The coefficients for the best fit in the lowest temperature range are $\alpha = 0.09 \pm 0.0085$ and $A = -315.1 \pm 11.1$ K (for $B = 16.33$ K). They can be compared to $\alpha = -0.04$ and $A = -8860$ K determined by Balberg and Maman [14] for dysprosium in the range $3 \times 10^{-4} < t < 3 \times 10^{-2}$. Theoretical prediction for A on Fermi wave vector, k_F, dependence has been done for simple bcc antiferromagnet [18]. A is positive for small k_F and exhibits an extremum of $A = -5.4$ K when the Fermi surface, FS, passes the magnetic Brillouin zone boundary, MBZB. Following Ref. [14] we consider the above data of α, A, and $t < 1.2 \times 10^{-2}$ for USb as a specific heat critical exponent, a critical amplitude of resistivity and a critical range, respectively.

A range of the mean field behaviour, yielding the $\rho \propto T^{1/2}$ dependence, is expected above the critical range. For USb, however, it is split into two parts: an intermediate range and the $\rho \propto t \ln t$ dependence range. The best fit in the intermediate range $1.15 \times 10^{-2} < t < 2.0 \times 10^{-2}$ gives $\alpha = 0.60 \pm 0.047$ and $A = -66 \pm 5.19$ K (also for $B = 16.33$ K). We consider this range as a residue of the mean field range where the resistivity behaviour is of the antiferromagnetic metal type [14].

The resistivity in the interval $2.0 \times 10^{-2} < t < 0.35$ is better described by the following equation:

$$R = At \ln t + Bt + C. \tag{2}$$

The best fit in this range gives $A = 81.9 \pm 1.8$ K, $B = 0 \pm 1.6$ K and $C = 240.6 \pm 0.26$ K. The theory predicts the same behaviour for semiconducting (or small k_F) ferromagnet. For the ferromagnet the centre of the Brillouin zone, BZ, is the magnetic instability point and small q fluctuations dominate at the critical temperature [20]. When temperature increases, a number of large q fluctuations increases at the expense of the small q ones. When their q vectors become larger than possible momentum transfer (i.e. $2k_F$) they cannot scatter the carriers effectively. It results in a decrease in magnetic resistivity according to $\rho \propto t \ln t$ relation.

The point of instability for antiferromagnet is at MBZB, therefore a large q dominated behaviour is expected in the vicinity of T_N. As T increases above T_N the small q fluctuations grow at the expense of the large q ones and resistivity of the antiferromagnetic metal decreases [14, 20] as t^{1-a} or $t^{1/2}$, in critical or mean field regions, respectively. For USb the existence of the small calliper FS sheet at MBZB, which presumably dominates the charge transport, is a possible reason for the observed small k_F ferromagnet-like behaviour of the resistivity. According to our knowledge the resistivity behaviour of semimetallic antiferromagnet having the small calliper of FS sheet at MBZB has not been analysed by theory and this is the first report of $\rho \propto t \ln t$ resistivity behaviour for antiferromagnet, suggesting some correspondence of this case to the semimetallic ferromagnet case.

The Fermi surface of semimetals consists both of electron and hole sheets. Its diffusion thermoelectric power S^e is given by

$$S^e = \sum_j (\sigma_j/\sigma) S_j^e, \tag{3}$$

σ_j and S_j^e are the electrical conductivity and the diffusion thermoelectric power of the particular sheet, respectively. We take j = h for hole sheets and j = e for the electron ones. The hole term is dominant for paramagnetic USb.

There are four formula units per unit cell of USb, i.e. one f.u. per BZ. The inset in Fig. 1 shows the energy bands along the [100] k-ray in the vicinity of the Fermi energy (E_F) according to Ref. [13].

When USb orders antiferromagnetically the magnetic moments of four uranium atoms in the crystal unit cell point along four different ⟨111⟩ directions. The magnetic lattice is then the simple cubic one with the framework containing 4 f.u. The magnetic BZ volume is four times smaller than BZ volume before ordering. MBZB cuts the paramagnetic BZ in the middle of the Γ–X line as shown by the vertical line (Q_i) in the inset in Fig. 1. As $(\sigma_j/\sigma)S_j^e$ might become dominant below T_S, an electron band having higher dispersion than a hole band should develop (presumably near MBZB) as temperature decreases below T_N.

4.2. Role of phonon drag

We discuss the origin of the 40 K maximum on the base of the well-known features of the phonon drag phenomenon [21, 22]. It contributes the $S^g(T)$ term having positive or negative peak at $T \approx (0.1 \div 0.3)\Theta_D$, where Θ_D is the Debye temperature. Above the temperature of the peak the $S^g \propto T^{-1}$ dependence is expected. Θ_D for some other monopnictides varies from about 260 K to about 360 K [1]. For a multi-sheet Fermi surface S may be expressed similarly by S^e (Eq. (3)), and

$$S = S^e + S^g; \qquad S^g = \sum_j (\sigma_j/\sigma) S_j^g. \tag{4}$$

Since a phonon scattering process induced by an impurity is "lost" for phonon drag thermoelectricity S^g is greatly reduced by the impurities and disorder.

We have analyzed the difference between the thermoelectric power behaviour for sample B, S^B, and that from Ref. [8], S^F. Within accuracy of reading S^F data

from Fig. 1 in Ref. [8] the $(S^F - S^B) \propto T^{-1}$ dependence was found in the range of $70 \div 140$ K. It implies that both samples have the same $S^e(T)$ but they differ by fraction of $S^g(T)$. We estimate that at about 40 K the contribution of S^g to S^B and S^F are higher than 50 μV/K and 5 μV/K, respectively.

An influence of phonon drag on electrical resistivity is a second order effect so the electrical resistivity is always reduced by phonon drag, ρ^g,

$$\rho^g = (S^g)^2 T/\lambda^g, \tag{5}$$

where λ^g is the lattice heat conductivity. We believe that the observed difference between the low temperature $\rho(T)$ dependence for samples A and B is caused mainly by the drag effect.

In order to expose this difference we have fitted the

$$\rho(T) = \rho_r + aT^n \tag{6}$$

expression to our experimental data by a nonlinear least squares sum method. The results are shown in Fig. 1. The exponent n is equal to $5/2 \pm 0.1$ (the residual resistivity, $\rho_r = 375.5 \pm 1.5$) for sample A and close to 4 for sample B ($n = 3.70 \pm 0.15$, $\rho_r = 47.8 \pm 1.4$). Schoenes et al. [5] reported earlier the $\rho \propto T^4$ behaviour for USb between *ca.* 10 K and 40 K and ascribed it to the scattering of the carriers on the spin waves of linear dispersion. However, a form of $\rho(T)$ dependence in the spin wave approximation depends on taking into account the various details of magnon dispersion and FS geometry [23]. For USb [24] as for UN [25] there is an apparent locking of the main magnetic response to the region of maximum phonon frequency. No theory of resistivity accounts for this feature, therefore we do not treat the interpretation of Ref. [5] as decisive and propose another one consistent with the interpretation of $S(T)$. It may also account for slightly negative temperature derivative of resistivity (hence minimum of resistivity) in the lowest temperature range shown in Fig. 4a.

The $\rho \propto T^{2.38}$ dependence is observed for ceramic UN [25] and $\rho \propto T^{5/2}$ dependence occurs for *ab* plane of monocrystalline USb_2 [16]. Therefore we have plotted resistivity data for samples A and B vs. (T/T_N) in the range *ca.* $2 \div 60$ K in Fig. 4b.

Solid straight lines present the best fit by the linear least squares sum method, where all plotted data for sample A and only the data indicated by arrows for sample B were used. In the latter case the data for $T < 45$ K show the negative deviation which we assume to be due to the phonon drag effect on resistivity. The concave curve is given by the expression from Fig. 1. The quantity $\rho^g(T)$, determined as the difference between straight and concave lines, has a maximum $\rho^g = 35$ $\mu\Omega$ cm at 33 K. Taking 50 μV/K for S^g, and using Eq. (5) we get the lattice heat conductivity $\lambda^g = 2.4 \times 10^{-3}$ W K^{-1} cm^{-1}. We note that the weighted sum for thermoelectric power Eq. (4) accounts for different signs of contributions while resistivity is lowered for each sign. Therefore, this approach underestimates the value of λ^g for USb. The most relevant of the available values of λ^g is the one for UN known only down to 80 K ($\lambda^g = 6.6 \times 10^{-2}$ W K^{-1} cm^{-1} [19]). We assume the $\lambda^g \propto T^3$ law for lower temperatures. This yields $\lambda^g = 4.6 \times 10^{-3}$ W K^{-1} cm^{-1} at 33 K, i.e. of the same order as estimated here for USb.

At 4.2 K the difference between resistivity of samples A and B is as huge as 330 $\mu\Omega$ cm, while the difference between resistivity of sample A and that of

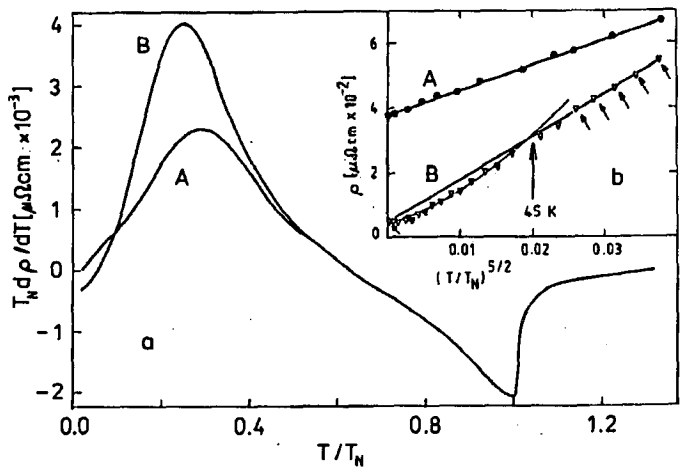

Fig. 4. The difference of the resistivity behaviour for examined samples A and B in terms of temperature derivative (a) and in the $[\rho, (T/T_N)^{5/2}]$ plot (b). The solid straight lines in (b) give linear fits to all data given by circles and only to data given by the triangles shown by arrows. The concave curve is given by the expression from Fig. 1.

Schoenes et al. [5] is equal to 285 $\mu\Omega$ cm. These differences decrease with increasing temperature and vanish near the resistivity maximum. Assuming that Matthiessen's rule is fulfilled, the difference can be ascribed to the additional contribution, ρ_{rm}, to the resistivity of sample A due to incoherent scattering of carriers. ρ_{rm} is presumably of magnetic origin as it is larger than the possible but unknown temperature independent residual resistivity, ρ_{ro}. The latter can be concluded from low RRR for sample B and inaccuracy of the room temperature resistivity.

The features attributed to phonon drag may also be due to the magnon drag. We think that magnon drag effects are dominant in USb because the diminishing of $S^g(T)$ seems to be connected mainly with ρ_{rm}.

5. Summary and conclusions

We have found that low temperature resistivity and thermoelectric power of uranium monoantimonide are very sample dependent and this phenomenon is related to stoichiometry variation. The single crystal characterized by $T_N = 218.7$ K and $RRR = 13$ shows a peak of thermoelectric power at 40 K, which is as high as about 50 μV/K. Such a gigantic peak of thermoelectric power was for the first time observed for USb and ascribed to magnon drag effect. This phenomenon explains also the presence of the resistivity minimum observed for crystals with high RRR. An increase in antimony to uranium content ratio decreases T_N, the lattice constant and RRR. This decrease in RRR is ascribed to incoherent scattering of carriers by magnetic disorder induced by stoichiometry deviation mainly.

The resistivity for the low RRR crystal shows $\rho \propto T^{5/2}$ dependence below 60 K in contrast to $\rho \propto T^4$ dependence observed below 40 K for the higher RRR

crystal. We show that the higher power resistivity dependence may be due to the magnon drag effect on resistivity.

The quantitative analysis of antiferromagnetic anomaly of resistivity gives the critical index $\alpha = 0.09$ and the critical amplitude $A = -315$ K proportional to electrical resistivity in the critical range $t = (T - T_N)/T_N \leq 1.15 \times 10^{-2}$. Resistivity decreases as $t \ln t$ in the range of $0.02 \leq t \leq 0.35$. We ascribe this type of behaviour, observed for the first time for semimetallic antiferromagnet, to the presence of the small calliper Fermi surface sheet at MBZB. The semimetallic features of USb structure are consistent with the presence of the high value of the magnon drag thermoelectric power as the latter is inversely proportional to the carrier concentration.

This work is devoted to Professor Robert Troć on the occasion of his 60th birthday anniversary.

References

[1] J.-M. Fournier, R. Troć, in: *Handbook on the Physics and Chemistry of the Actinides*, Eds. A.J. Freeman, G.H. Lander, Vol. 2, North-Holland, Amsterdam 1985, p. 29.

[2] J.-M. Fournier, E. Gratz, in: *Handbook on the Physics and Chemistry of Rare Earths*, Eds. K.A. Gschneider, Jr., L. Eyring, G.H. Lander, G.R. Choppin, Vol. 17, Chap. 115, North-Holland, Amsterdam 1993, pp. 409–537.

[3] B.R. Cooper, Q.G. Sheng, S.P. Lim, *J. Alloys Compd.* **192**, 223 (1993); B.R. Cooper, in: *Abstracts of Europ. Conf. Physics of Magnetism '93, Strongly Correlated Systems, Poznań 1993*, Ed. A. Wójtowicz, OWN, Poznań 1973, p. 13.

[4] J. Rossat-Mignod, P. Burlet, S. Quézel, O. Vogt, *Physica B* **102**, 237 (1980).

[5] J. Schoenes, B. Frick, O. Vogt, *Phys. Rev. B* **30**, 6578 (1984).

[6] B. Frick, J. Schoenes, O. Vogt, *J. Magn. Magn. Mater.* **47&48**, 549 (1985).

[7] W. Reim, J. Schoenes, O. Vogt, in: *Proc. 14 Journées des Actinides, Davos 1984*, Ed. J. Schoenes, ETH, Zürich, p. 34.

[8] B. Frick, J. Schoenes, O. Vogt, in: *Program, Abstracts 15 Journées des Actinides, Liège 1985*, Ed. J. Fuger, University of Liège, p. 114.

[9] A. Ochiai, Y. Suzuki, T. Shikama, K. Suzuki, E. Hotta, Y. Haga, T. Suzuki, *Physica B* **199&200**, 616 (1994).

[10] E. Hotta, A. Ochiai, Y. Suzuki, T. Shikama, K. Suzuki, Y. Haga, T. Suzuki, *J. Alloys Compd.* **219**, 252 (1995).

[11] Z. Henkie, P.J. Markowski, *J. Cryst. Growth* **41**, 303 (1977).

[12] Z. Henkie, P.J. Markowski, A. Wojakowski, Ch. Laurent, *J. Phys. E, Sci. Instrum.* **20**, 40 (1987).

[13] R. Podloucky, P. Weinberger, *Physica B* **102**, 59 (1980).

[14] I. Balberg, A. Maman, *Physica B* **96**, 54 (1979).

[15] E. Pleska, J.-M. Fournier, J. Chiapusio, J. Rossat-Mignod, J. Rebizant, J.C. Spirlet, O. Vogt, in: *20 Journées des Actinides 1990*, V. Sechovsky, Charles University, Prague.

[16] Z. Henkie, R. Maślanka, P. Wiśniewski, R. Fabrowski, P.J. Markowski, J.M. Franse, M. van Sprang, *J. Alloys Comp.* **181**, 267 (1992).

[17] Z. Henkie, P. Wiśniewski, R. Fabrowski, R. Maślanka, *Solid State Commun.* **79**, 1025 (1991).

[18] T.G. Richard, D.J.W. Geldart, *Phys. Rev. B* **15**, 1502 (1977).

[19] J.P. Moore, W. Fulkerson, D.L. McElroy, *J. Amer. Ceram. Soc.* **53**, 76 (1970).

[20] I. Balberg, *Physica B* **91**, 71 (1977).

[21] R.P. Huebener, *Solid State Phys.* **27**, 63 (1972).

[22] F.J. Blatt, P.A. Schroeder, C.L. Foiles, D. Greig, *Thermoelectric Power of Metals*, Plenum Press, New York 1976.

[23] K. Ueda, *J. Phys. Soc. Jpn.* **43**, 1497 (1977).

[24] G.H. Lander, W.G. Stirling, *Phys. Rev. B* **21**, 436 (1980).

[25] T.M. Holden, W.J.L. Buyers, E.C. Svensson, G.H. Lander, *Phys. Rev. B* **30**, 114 (1984).